Supplementary Figure 1

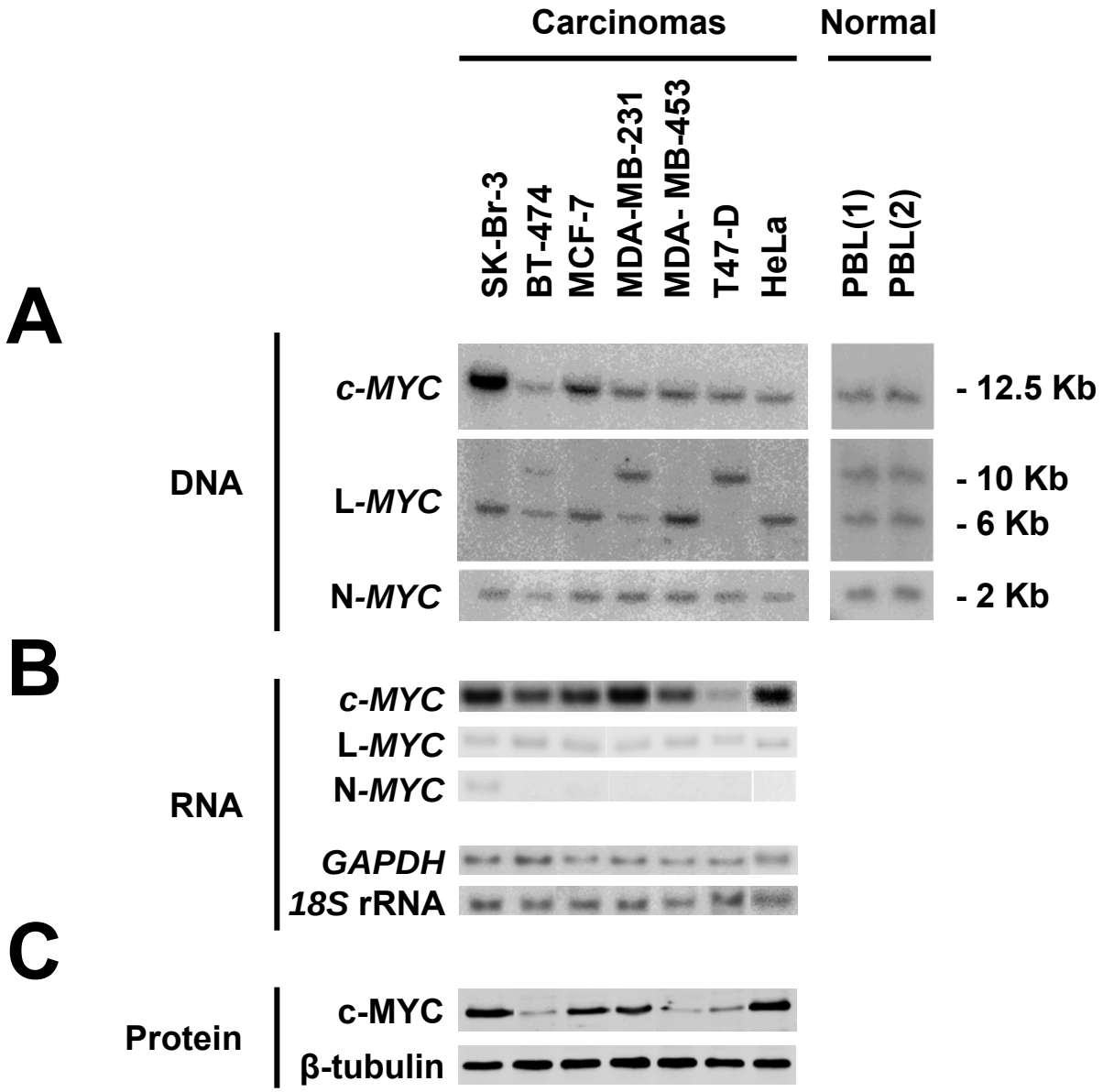

Supplementary Fig. 1: Genomic status and expression levels of *MYC* genes in human carcinoma cells.

(A) Southern blot analysis of *Eco*RI digested genomic DNA isolated from normal peripheral blood leukocytes (PBL) and human carcinoma cell lines using c-*MYC*, L-*MYC* and N-*MYC* probes. High copy amplification (36 copies) of c-*MYC* is observed in SK-Br-3 cells, and low copy amplification (8 copies) of c-*MYC* is found in MCF-7 breast cancer cells. L-*MYC*, which shows a restriction fragment length polymorphism, and N-*MYC* are not amplified in these carcinoma cells.
(B) Quantitative radioactive reverse transcription-polymerase chain reaction analysis of c-*MYC*, L-*MYC* and N-*MYC* mRNA levels in human carcinoma cell lines. c-*MYC* is expressed at high levels, except in T47-D; L-*MYC* is expressed at low levels, and N-*MYC* transcripts, with the exception of SK-Br-3 cells, are generally undetectable. *GAPDH* (glyceraldehyde-3-phosphate dehydrogenase) mRNA and *18S* rRNA were used for normalization.
(C) Western blot analysis of c-MYC protein in human carcinoma cell lines. β-tubulin analysis of the same extracts was used as a control for protein loading.

Supplementary Figure 2

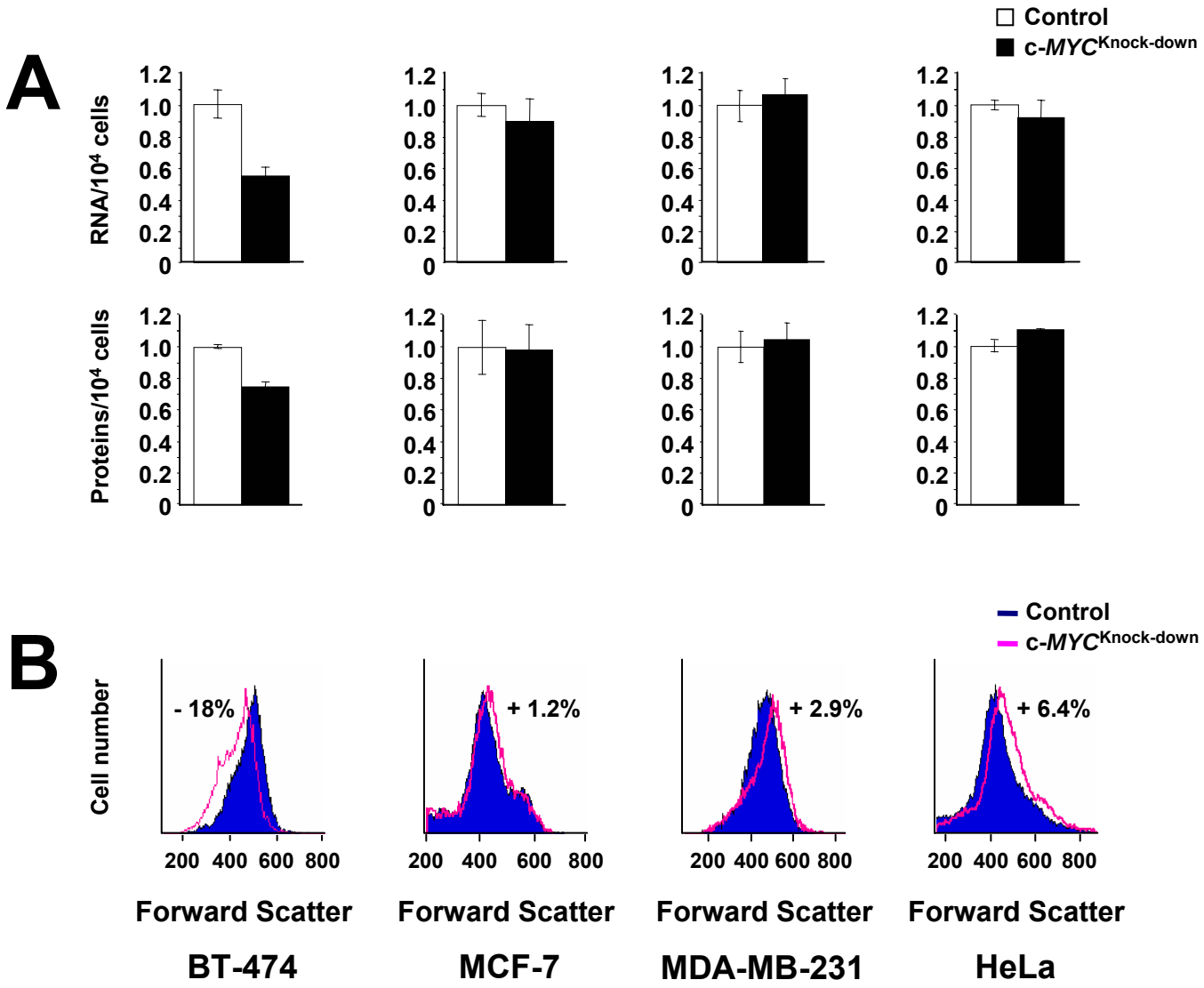

Supplementary Fig. 2: c-MYC depletion results in altered global RNA and protein content as well as cell size in BT474 breast carcinoma cells but not other cell lines.

Human carcinoma cells were transfected with control and c-*MYC*^{KD} (knock-down) siRNA and analyzed 3 days later.

(*A*) Total RNA and protein content in control (white bars) and c-MYC depleted cells (black bars). Cells were harvested and counted, and RNA and proteins were extracted from the same number of control and c-MYC depleted cells. RNA and protein yields are expressed relative to the value from control cells. The plotted values are the means of three independent replicates, and errors bars represent Standard Error of the Mean (SEM).

(*B*) Cell size was analyzed by flow cytometric analysis of forward scatter (FSC) distribution. A representative example is displayed for each cell line and values represent FSC changes in c-MYC depleted relative to control cells. Blue curves: control cells; Pink curves: c-MYC depleted cells.

Supplementary Figure 3

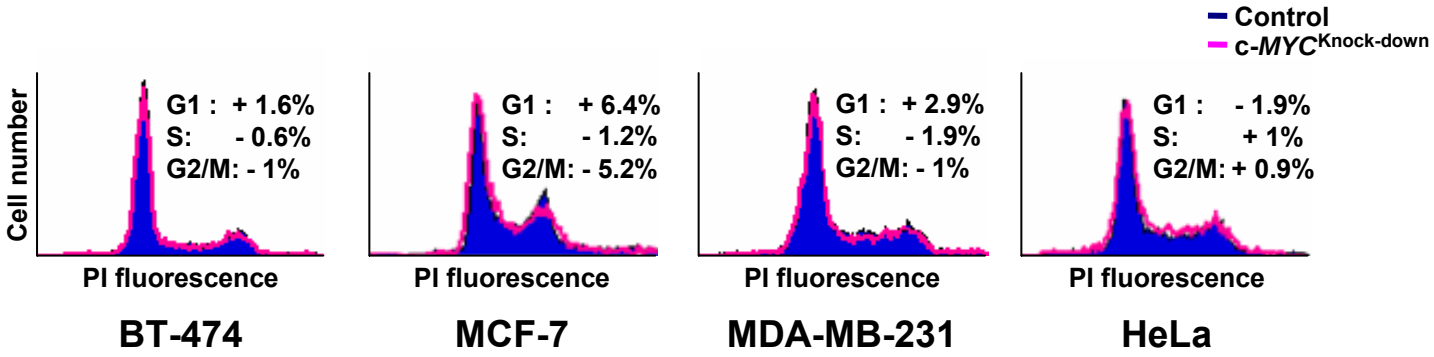

Supplementary Fig. 3: Effects of c-MYC down-regulation on cell cycle distribution and cell death.

Cells were transfected with control and c-*MYC*^{KD} (knock-down) siRNA and analyzed 3 days later for cell cycle distribution by flow cytometric measurement of propidium iodide (PI) staining. A representative example is displayed for each cell line and values represent cell cycle changes in c-MYC depleted (pink curves) relative to control cells (blue curves). c-MYC depleted cells showed very limited changes in the cell cycle distribution, with no checkpoint defect and no evidence of cell death.

Supplementary Figure 4

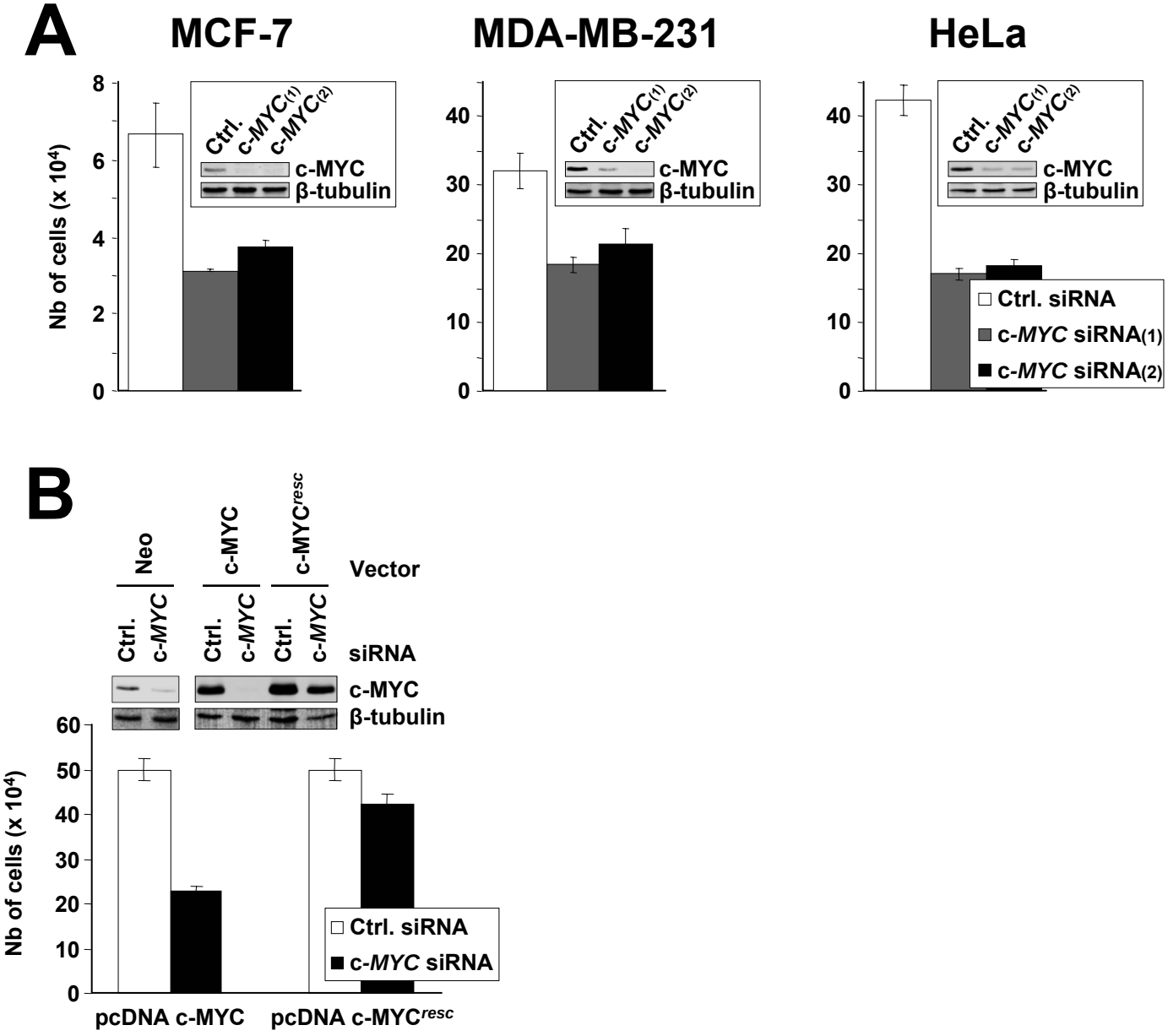

Supplementary Fig. 4: c-*MYC* siRNAs exert specific effects.

(A) The specificity of c-*MYC* small interfering RNA (siRNA) was controlled by testing the anti-proliferative effects of 2 siRNA targeting different regions of c-*MYC* mRNA. Cells were counted 3 days after c-MYC^{KD} (knock-down) and control siRNA transfection. Plotted values are the means of three replicates, and errors bars represent standard error of the mean (SEM). Both siRNA led to a similar inhibition of MCF-7, MDA-MB-231 and HeLa cell proliferation, indicating that those effects are independent of the siRNA sequence. The down-regulation of c-MYC by siRNA was verified by Western blotting, β-tubulin analysis of the same extracts was used as a control for protein loading (insert).
(B) To further control the specificity of c-MYC siRNA, constructs encoding wild-type c-MYC (c-MYC), a c-*MYC* allele rendered resistant to one of the siRNA (c-MYC^{resc}) by introduction of a silent mutation, and the empty vector (Neo) were transiently co-transfected in HeLa cells together with control (Ctrl.) and c-*MYC* siRNA. Transfected cells were harvested 3 days later. c-MYC protein levels were determined by Western blotting (β-tubulin analysis of the same extracts was used as a control for protein loading), and cells were counted for proliferation analysis. The c-MYC^{resc} construct could rescue c-MYC levels and the proliferation defect resulting from c-*MYC* siRNA, proving that the block of proliferation is due to c-MYC knock-down and not to off target effects.

Supplementary Figure 5

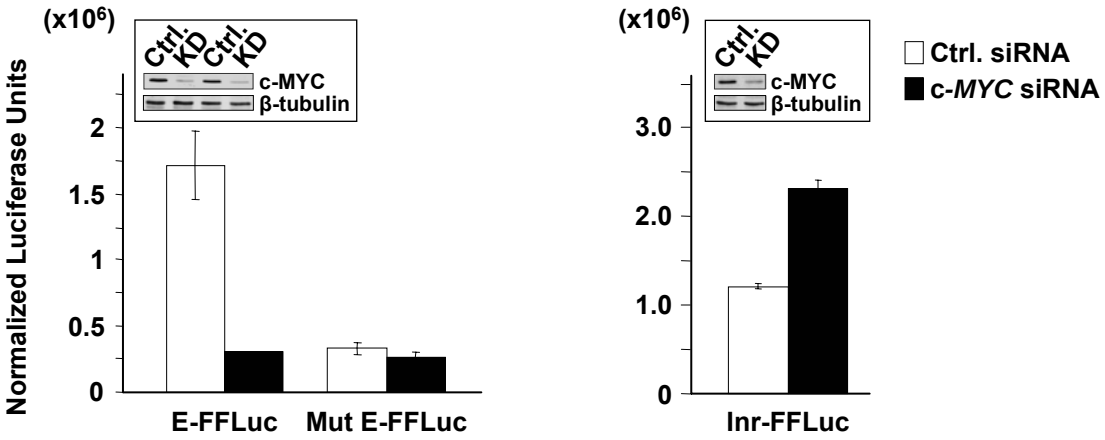

Supplementary Fig. 5: c-*MYC* siRNAs alter MYC-regulated transcription.

Effects of c-MYC down-regulation on MYC-regulated transcription were examined by reporter gene analysis. Wild-type (E-FF-Luc) and mutant (Mut E-FF-Luc) E-box- and Initiator elements (Inr-FF-Luc) (*CDKN1a* promoter)-driven Firefly Luciferase reporter constructs were co-transfected in HeLa cells together with control (Ctrl.) and c-*MYC* (KD) small interfering RNA (siRNA). A co-transfected SV-40-Renilla Luciferase construct was used to normalize for plasmid transfection efficiency. Cells were harvested 3 days after transfection. Transcriptional activity is plotted as normalized Firefly Luciferase activity. Values are the means and standard error of the means (s.e.m.) of three replicates. The down-regulation of c-MYC by siRNA was verified by Western blotting, and β-tubulin analysis of the same extracts was used as a control for protein loading (insert). These experiments showed that c-MYC depletion affects MYC-dependent transcription, with E-box activity (positively regulated by MYC) being repressed, as previously reported (Von der Lehr N *et al.* (2003) The F-box protein Skp2 participates in c-MYC proteosomal degradation and acts as a cofactor for c-Myc-regulated transcription. *Mol. Cell* **11**: 1189-1200) and Inr activity (negatively regulated by MYC) being stimulated.

Supplementary Figure 6

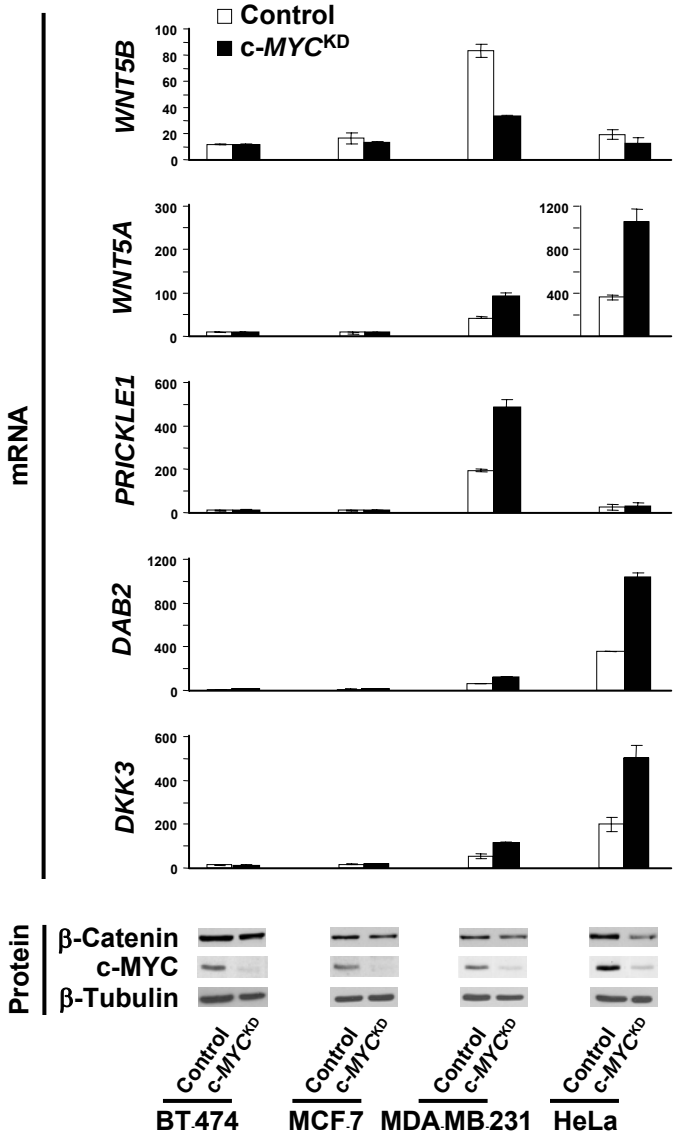

Supplementary Fig. 6: c-MYC exerts a positive transcriptional feed-back on WNT signaling contributing to proliferation in MDA-MB-231 and HeLa cells.

Microarray expression profiles (Mean ± SEM from independent replicates) of WNT pathway genes in control and c-*MYC*^{KD} (knockdown) cells. In MDA-MB-231 and HeLa cells, c-MYC depletion leads to up-regulation up-regulation of *WNT5A*, which acts as a tumor suppressor gene in certain cancers (Liang *et al.* (2003) Wnt5a inhibits B cell proliferation and functions as a tumor suppressor in hematopoietic tissue. *Cancer Cell* **4**: 349-360), and of *DAB2* and *DKK3*, which encode canonical WNT signaling antagonists (Hocevar *et al.* (2003) Regulation of the Wnt signaling pathway by disabled-2 (Dab2). *EMBO J.* **22**: 3084-3094; Hoang *et al.* (2004) Dickkopf 3 inhibits invasion and motility of Saos-2 osteosarcoma cells by modulating the Wnt-beta-catenin pathway. *Cancer Res.* **64**: 2734-2739). c-MYC depleted MDA-MB-231 cells also display up-regulation of *PRICKLE1*, encoding another putative canonical WNT pathway antagonist (Jenny *et al.* (2005) Diego and Prickle regulate Frizzled planar cell polarity signaling by competing for Dishevelled binding. *Nat. Cell Biol.* **7**: 691-697, and references therein), and down-regulation of *WNT5B*, encoding a candidate oncogenic ligand (Lu *et al.* (2004) Activation of the Wnt signaling pathway in chronic lymphocytic leukemia. *Proc. Natl. Acad. Sci. USA* **101**: 3118-3123). Western blotting confirmed c-MYC knockdown by small interfering RNA (siRNA) and revealed down-regulation of β-catenin levels in HeLa cells. β-Tubulin was included as a loading control.

Supplementary Figure 7

A

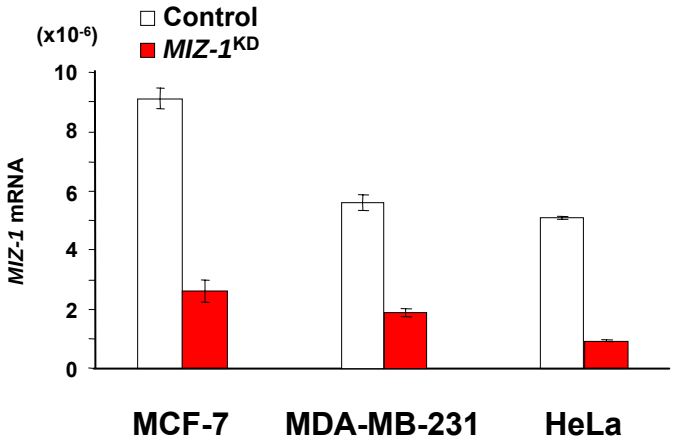

B

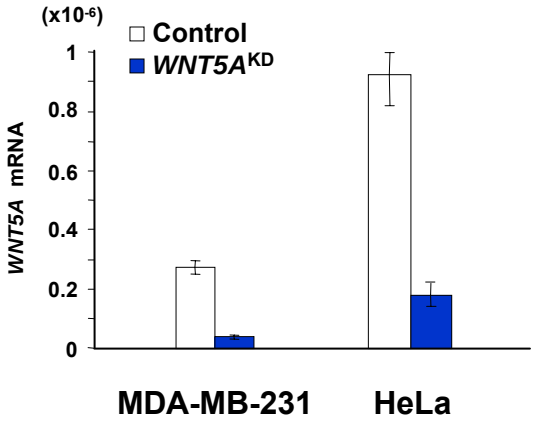

Supplementary Fig. 7: Efficiency of *MIZ-1* and *WNT5A* siRNA-mediated silencing.

RNA from the indicated cell lines were collected 3 days after Control, *MIZ-1*^{KD} (knockdown) or *WNT5A*^{KD} siRNA transfection, and assayed for *MIZ-1* or *WNT5A* gene inhibition. Quantitative real-time RT-PCR analyses of *MIZ-1* (***A***) and *WNT5A* (***B***) mRNA levels, normalized by *18S* rRNA (Mean ± SEM from independent measurements) are shown. Normalization by *EF1-α* (elongation factor 1-alpha) mRNA gave similar inhibition (not shown). MIZ-1 and WNT5A protein levels could not be analyzed due to the lack of sensitivity of available antibodies to detect endogenous levels in the studied cells.

Supplementary Figure 8

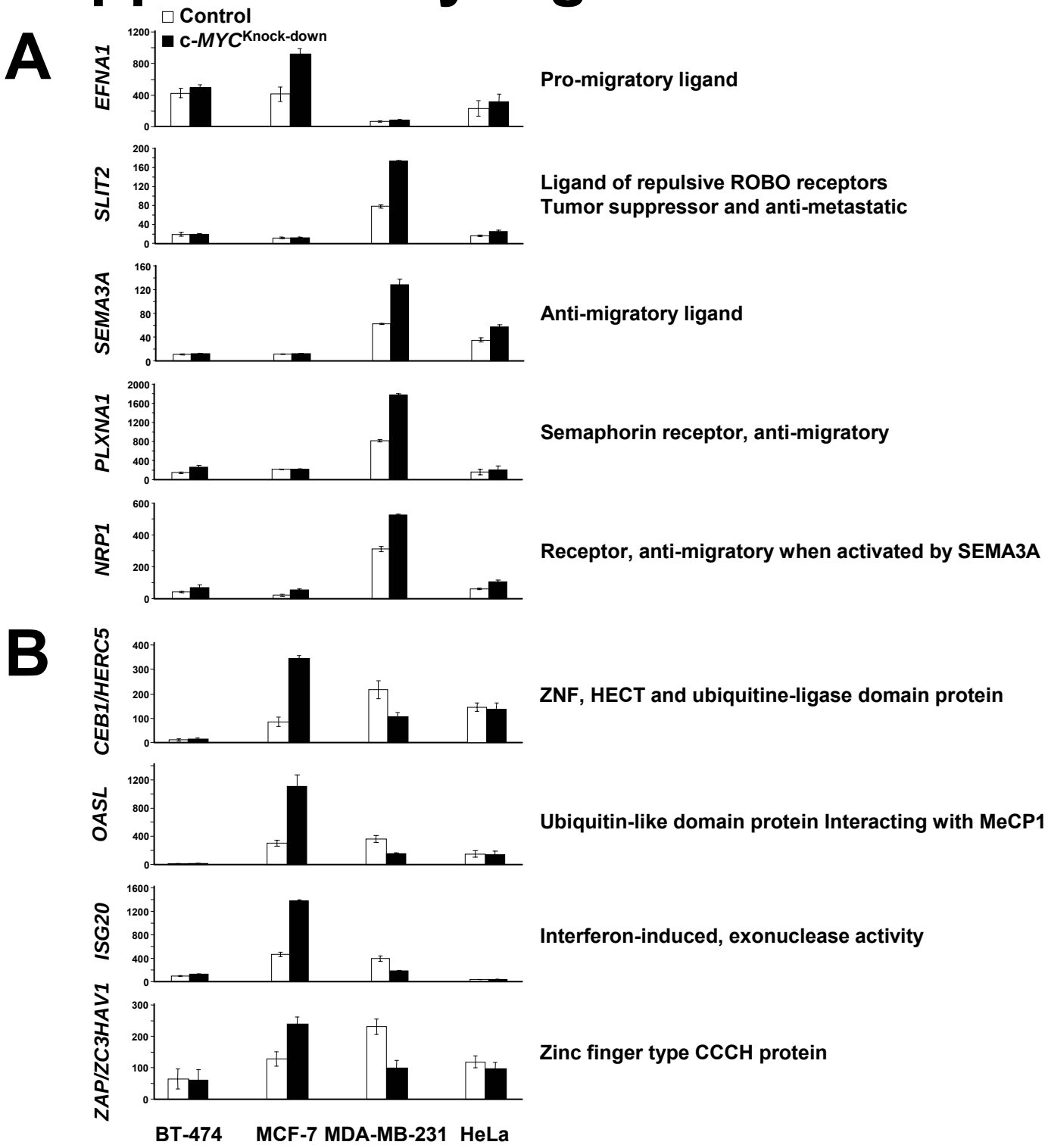

Supplementary Fig. 8: c-MYC targets whose regulation correlates with effects of c-MYC depletion on cell migration.

(A) Microarray expression profiles (Mean ± SEM from independent replicates) showing that genes whose products are known to either promote or inhibit cell migration are induced, respectively, in MCF-7 or MDA-MB-231 c-*MYC*^{KD} (knockdown) cells. ***(B)*** Others, with no established function, are up-regulated in MCF-7 and repressed in MDA-MB-231 c-*MYC*^{KD} cells, which respectively show increased and reduced migration in response to c-MYC depletion **(Fig. 1D)**.